

# Improvement of mechanical properties, microscopic structures, and antibacterial activity by Ag/ZnO nanocomposite powder for glaze-decorated ceramic

Qian ZHANG, Lv Si XU\*, Xiaoyan GUO

College of Chemical Engineering, Huaqiao University, Xiamen, China

Received: March 15, 2017; Revised: June 06, 2017; Accepted: July 13, 2017

© The Author(s) 2017. This article is published with open access at Springerlink.com

**Abstract:** With the increase in the international trade of ceramics, improvement in the physical and chemical properties of ceramics has become a market demand in recent years. The addition of nanomaterials in glaze can simultaneously improve the mechanical and corrosion resistance properties of ceramics. In this study, the effect of nano-sized Ag/ZnO in glazed ceramic was investigated considering the hardness, whiteness, and microscopic structures of the products. Results showed that the Ag/ZnO nanocomposite powder significantly affects the performance of glaze. Glaze hardness reached the highest value (96.6 HV) at the low sintering temperature of 1130 °C with the addition of 10% Ag/ZnO nanocomposite powder. Furthermore, the Ag/ZnO nanocomposite powder improved crack resistance and whiteness. Ag as AgO and Ag<sub>2</sub>O in the glaze was effective for antibacterial activity of ceramic. In addition, the Ag/ZnO nanocomposite powder could also promote the shrinkage of bubbles in the glaze layer and smooth the glaze. These results indicated that the nanoparticles could act as an active center for melting raw materials, which is crucial for ceramic properties.

**Keywords:** Ag/ZnO nanocomposite powder; sintering temperature; performance; microstructure; antibacterial activity

## 1 Introduction

Ceramic is an attractive and excellent product for a wide range of applications. Unfortunately, the ceramic industry involves high energy consumption, resource waste, serious pollution, and inferior quality of products. For further development, energy conservation and environmental protection have become the focus of the ceramic industry. The application of nanomaterials in ceramic preparation has gained significant attention since it was first reported by Niihara *et al.* given their

high strength, high surface hardness, excellent ductility, and toughness [1–3]. Currently, in the field of ceramics, the addition of nanomaterials not only improves the mechanical properties of ceramics but also provides special functions [2,3]. For example, the addition of Ag ions can greatly improve the antimicrobial properties and self-clean ability of ceramics. Since silver ions can interact with bacterial cells in ways below: (1) interacting with microbial DNA to inhibit replication or cause protein denaturation; (2) inhibiting cells respiration and preventing the important substances passing through the membrane into the cell [4]. However, the transfer of Ag ions to Ag atoms under high sintering temperature can lead to loss of antibacterial activity and oxidation discoloration, which

\* Corresponding author.  
E-mail: xls895623@126.com

greatly inhibit its application.

Many scholars have attempted to coat Ag ions into glass and ceramics. In the research of Kawashita *et al.* [5], the ratio of Al and Ag was controlled in silver-containing silica glass to simulate the color and release rate of silver ions. Such Ag–silica glass powder with compositions of Al/Ag > 1 is suspected to contribute to the color and antibacterial activity of the material. For the mechanism, the aluminum ion possibly existed as the form of  $[\text{AlO}_4]^-$  tetrahedra in the  $\text{SiO}_2$  structure, and its negative charge was compensated by  $\text{Ag}^+$  ion. Consequently, the  $\text{Ag}^+$  ion is combined with the  $[\text{AlO}_4]^-$  tetrahedra and hard to be transferred into metallic silver [5]. The existences of  $\text{Ag}^+$  lead to high antibacterial activity and whiter color. The effect of  $\text{AgNO}_3$  organic–inorganic hybrid solutions on the antibacterial behavior of a typical soda-lime slide glass was investigated by Lee *et al.* [6]. This coating film exhibited excellent antibacterial activity for both *Staphylococcus aureus* (> 99.99%) and *Escherichia coli* (> 99.99%). The antibacterial activity in this research was corresponding to the Ag ion releasing, which ions were exchanged by  $[\text{H}_3\text{O}]^+$  [6]. In 2012, Nafiseh and his co-workers prepared silver-doped silica thin films on the glazed surface of ceramic tiles by sol–gel method to achieve antibacterial activity. These coated films show 100% antibacterial activity against both *E.coli* and *S.aureus* [7]. In most recent research of Liu *et al.* [8], a ceramic-like surface structure with the addition of Ag–Si–polyamine 66 complex was prepared and exhibited strong antibacterial activity (> 99.99%), since the ionic state Ag (rather than metallic Ag) was bond with oxygen atoms in the carboxyl group of polyamine 66. The hardness of the material was 0.45–0.7 GPa. The researching results of Li *et al.* [9] indicated that  $\text{Zn}^{2+}$  is favorable for maintaining the silver in the form of the ionic form, and improving the anti-discoloration properties of Ag. The existence of ZnO also improved the fusible properties, flexible

properties, mechanical strength, and thermal stability of the glaze, in order to enhance the whiteness and gloss of glaze and widen the preparation conditions under proper loading [9]. In summary, the properties of ceramic with Ag contained nanomaterial addition greatly depended on the microstructure and chemical states of Ag and nanomaterials, no matter the loading position of framework or surface. The properties of some nanomaterial loaded ceramics are listed in Table 1 [8,10–15].

To further describe the performance of Ag-containing nanomaterials in ceramic, this study fabricated glaze-decorated ceramic with the addition of nano-sized Ag/ZnO. Properties including crack resistance, whiteness, mechanical properties, microscopic structures, and antibacterial activity were investigated and discussed in detail. Results indicated that the addition of Ag/ZnO nanocomposite positively affects the reduction in melting temperature of feldspar to decrease sintering temperature. The antibacterial property of glaze-decorated ceramics indicated excellent antibacterial activity against *E.coli* because of the existence of AgO and  $\text{Ag}_2\text{O}$ .

## 2 Experiment

### 2.1 Chemicals

Ceramic clay and glaze used in this research were purchased from Dehua Company (Quanzhou, China).  $\text{AgNO}_3$  and  $(\text{NaPO}_3)_6$  were purchased from LvYin Company (Xiamen, China) with purity of 99.99%. The main components in the raw materials were analyzed by energy dispersive spectroscopy (EDS), as shown in Table 2. According to the classification of the mineral composition of raw materials, glaze was mainly composed of potassium feldspar ( $\text{K}_2\text{O}\cdot\text{Al}_2\text{O}_3\cdot 6\text{SiO}_2$ ), sodium feldspar ( $\text{Na}_2\text{O}\cdot\text{Al}_2\text{O}_3\cdot 6\text{SiO}_2$ ), calcium feldspar ( $\text{Ca}_2\text{O}\cdot\text{Al}_2\text{O}_3\cdot 6\text{SiO}_2$ ), celsian ( $\text{BaO}\cdot\text{Al}_2\text{O}_3\cdot 6\text{SiO}_2$ ),

**Table 1 Properties of some nanomaterial-loaded ceramics**

Material	Hardness	Color/whiteness	Antibacterial activity	Ref.
20.0–36.5 wt% $\text{Y}_2\text{O}_3$ added ceramic	370–1010 HV			[10]
Si–Ag–polyamine 66 added ceramic-like structure	0.45–0.7 GPa		<i>E.coli</i> >99.98%	[8]
$\text{Yb}^{3+}:\text{Y}_2\text{O}_3$ ceramic	8.65 GPa			[11]
Ultrafine silver(II) oxide particles decorated porous ceramic composites		Black	<i>E.coli</i> >99.94%	[12]
Ag–3D-glass–ceramic		Gray	2–3 mm	[13]
Silver nanoparticle decorated porous ceramic		Brown	10 mm	[14]
Ag decorated $\text{TiO}_2$ photocatalytic membrane		Brown	27 mm	[15]
Ag/ZnO decorated ceramic	>95 HV (>3.2 GPa)*	White (whiteness >78)	2–3 mm	This research

\*Calculated by the equation of  $\text{HV} = 0.189F/d^2$ , in which  $d$  is equal to 0.08 mm.

**Table 2** Components in the raw clay and glaze

Component	SiO <sub>2</sub>	Al <sub>2</sub> O <sub>3</sub>	K <sub>2</sub> O	MgO	CO <sub>2</sub>	CaO	BaO	Na <sub>2</sub> O
Clay	76.67%	18.57%	4.19%	0.57%	—	—	—	—
Glaze	35.8%	6.7%	2.7%	0.68%	41.96%	5.68%	4.87%	1.62%

clayey(SiO<sub>2</sub>, Al<sub>2</sub>O<sub>3</sub>), calcite (CaCO<sub>3</sub>), dolomite (MgCO<sub>3</sub>·CaCO<sub>3</sub>), magnesite (MgCO<sub>3</sub>), high bauxite (kaolinite Al<sub>2</sub>O<sub>3</sub>·2SiO<sub>2</sub>·2H<sub>2</sub>O, and diaspor), and sillimanite (Al<sub>2</sub>O<sub>3</sub>·SiO<sub>2</sub>).

## 2.2 Preparation of Ag/ZnO nanoparticles

In this research, silver nitrate was used as Ag precursor and zinc sulfate was used as Zn precursor. During reaction, certain amount of silver nitrate (AgNO<sub>3</sub>, 99%) was mixed with 0.2 g zinc sulfate (ZnSO<sub>4</sub>·7H<sub>2</sub>O, 99%) within 150 mL DI water in 250 mL container. For the optimization of Ag/ZnO preparation, pre-experiment has been carried out on various Ag/ZnO ratio (0.05:1, 0.01:1, 0.1:1), heating temperature (400, 500, 600 °C) under different time (3.0, 2.0, 1.5, 1.0, 0.5 h). The result shows that the most stable material can be achieved under the Ag/ZnO ratio of 0.05:1, heating temperature of 500 °C with 0.5 h. Furthermore, the sintering was carried out under ambient atmosphere. In this research, the Ag/ZnO molar ratio was all controlled at 0.05:1. Oxalic acid solution was then dispersed in the previous solution by continuous stirring. After 30 min reaction, the product was collected by filtration, aging, washing by ethanol, and subsequent drying at 105 °C for 2 h. After calcination at 500 °C for 30 min, the final products of Ag/ZnO nanoparticles were obtained. The as-synthesized Ag/ZnO was white colored particles.

## 2.3 Preparation of glazed ceramic

For glazed ceramic preparation, the clay was firstly shaped to the size of 3 cm × 3 cm × 0.15 cm by the mould. Then the ceramic was obtained after sintering of 900 °C. The Ag/ZnO power was mixed with sodium hexametaphosphate to enhance the dispersion status of nanoparticles and then used to glaze the pre-prepared ceramic sheets by 20 mL. The final glazed ceramic was obtained after sintering.

## 2.4 Antibacterial test

The antibacterial property of glaze-decorated ceramics was analyzed by *E.coli* (ATCC:25922). For glazed ceramic preparation, the clay was firstly shaped to the size of 3 cm × 3 cm × 0.15 cm by the mould. Then the ceramic was located in the center of medium that is full

of *E.coli*. The inhibition width around ceramic after 48 h culture was measured by vernier caliper.

## 2.5 Characterization of Ag/ZnO nanoparticles and glazed ceramic

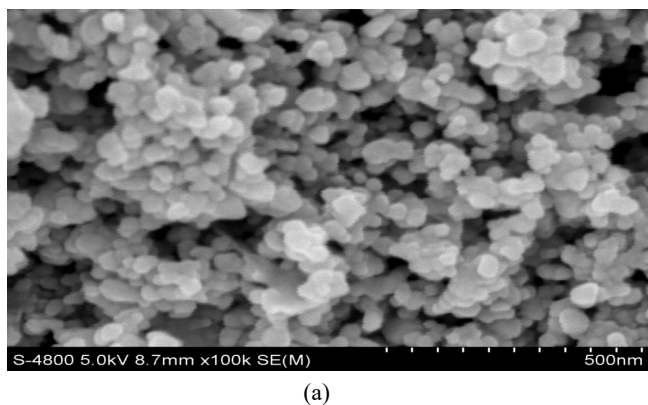
Components in the raw materials of glaze and ceramic were analyzed by EDS (7021, Oxford Instruments). The hardness and whiteness of the products were analyzed by Vickers hardness tester (HS-19GD, API) and color spectrum chromatic meter (TAS990, Purkinje), respectively. A thermogravimetric analyzer (TGA, TADSC2910/SDT2960, SHIMADZU) was used to identify weight loss in the sintering process. Crack resistance analysis was carried out by an autoclave to increase the pressure to 500 MPa and then decrease rapidly in 30 min. After the rapid change in pressure, the samples were observed with methylene blue. For microscopic structure analysis, the glaze materials with added ZnO or Ag/ZnO were prepared and then used to glaze the round ceramic sheets (Φ 15 mm) by 20 μL. The ceramic sheets were sintered under 1150 °C with a holding time of 10 min. X-ray photoelectron spectroscopy (XPS, Auger, ESCA) was used to analyze the components and valence of Ag. The microscopic structures of glazed ceramic were then analyzed by a scanning probe microscope (S-3500N, HITACHI) and polarizing microscope (PMS-201, EMBOSSSED). The crystal phase of Ag/ZnO nanoparticles was identified by X-ray powder diffractometer (XRD, D8 Advance).

## 3 Results and discussion

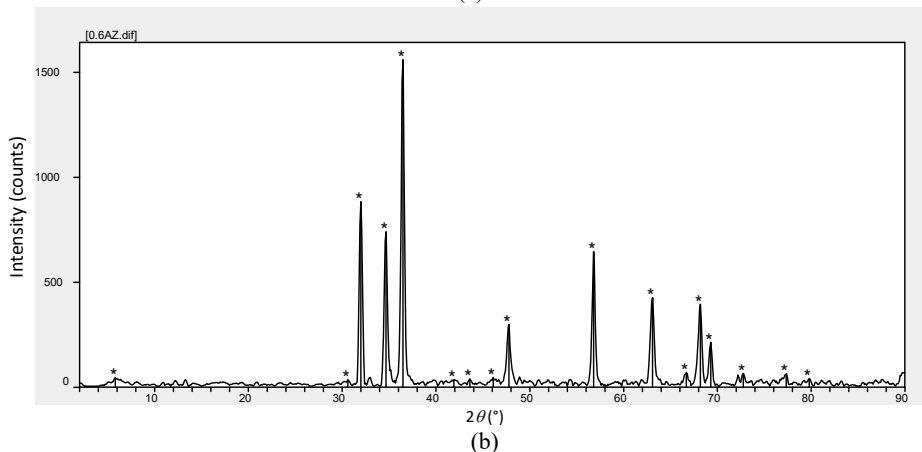
### 3.1 Characterization of Ag/ZnO nanoparticles

The characterization of Ag/ZnO nanoparticles was crucial for the properties of ceramic. The surface morphology of the prepared Ag/ZnO nanocomposite was shown in Fig. 1(a). As shown, the spherical particle of Ag/ZnO nanocomposite can be observed clearly with size range of 20–60 nm. This phenomenon indicated the average loading of Ag components on the ZnO surface without agglomeration.

To further analyze the crystalline nature of the nanomaterial, XRD has also been employed (as shown in Fig. 1(b)). The XRD analysis shows various Bragg



(a)



(b)

**Fig. 1** (a) SEM image of Ag/ZnO nanocomposite powder; (b) XRD patterns of Ag/ZnO nanocomposite powder.

reflections at 32.0°, 34.7°, 36.5°, 47.9°, 56.8°, 63.1°, and 68.2°, corresponding to the (100), (002), (101), (102), (110), (103), (112) sets of lattice planes [16,17]. The XRD JCPDS Card was No. 36-1451. The appearance of those Bragg reflections indicated the face centered cubic ZnO nanoparticles [16]. The small Bragg's reflections at 46.2° were attributed to the face centered cubic silver [18] (JCPDS Card No. 04-0783). This phenomenon confirmed the anchoring of Ag onto ZnO particles.

**3. 2 Effect on mechanical properties**

The hardness of glazed ceramic is an important mechanical property of ceramics. Given that it is significantly affected by the sintering temperature and holding time, these two parameters were analyzed in this research. With 0%, 3%, 5%, 7%, and 10% Ag/ZnO loading, hardness was analyzed by changing the sintering temperature from 1050 to 1190 °C under 10–30 min holding time. As shown in Fig. 2, with the increase in sintering temperature without Ag/ZnO loading, the hardness of the glaze continuously increases. When the sintering temperature is below

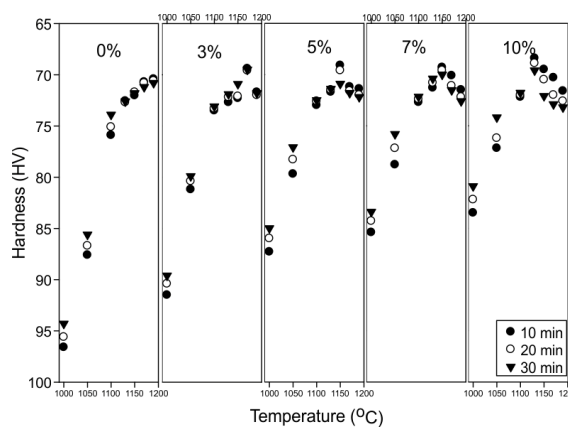


**Fig. 2** Influence of hardness on ceramic glaze by Ag/ZnO nanocomposite powder.

1150 °C, the hardness of the glaze increases with the holding time under the same sintering temperature. When the sintering temperature is higher than 1170 °C, hardness slightly decreases with the extended holding time. The extended holding time is beneficial for the flexibility of the glaze. When the sintering temperature is 1170 °C with 10 min holding time, hardness reached the maximum value of 94.6 HV. With the addition of Ag/ZnO (as shown in Fig. 2), the hardness of glazed

ceramics increases with the increase in sintering temperature and extended holding time under relatively low sintering temperature. Under high sintering temperature, hardness also initially increases with the sintering temperature but gradually decreases with the extended holding time. To further analyze the effect of different sintering temperature and Ag/ZnO loading, the hardness under sintering temperature of 1190–1130 °C with 0%–10% Ag/ZnO loading was investigated. The result shows that the maximum hardness under different conditions were 94.6 (1190 °C, 0%, holding time 10 min), 95.6 (1170 °C, 3%, holding time 10 min), 95.9 (1150 °C, 5%, holding time 10 min), 95.7 (1150 °C, 7%, holding time 10 min), and 96.6 (1130 °C, 10%, holding time 10 min), respectively. The result obviously indicates that the addition of the Ag/ZnO nanocomposite powder is beneficial for the sintering of ceramic. With the increase in the Ag/ZnO content, high surface hardness of glazed ceramic is achieved under low sintering temperature.

To further confirm the decrease in sintering temperature with Ag/ZnO loading, the thermal stability of 0%, 3%, 5%, and 7% Ag/ZnO-loaded glazed ceramic samples was analyzed in nitrogen atmosphere with a carrier gas flow rate of 50 mL/min and temperature rising rate of 15 °C/min. Pure Ag/ZnO (marked as AZ) was analyzed as a contrast, and the thermogravimetric analysis (TGA) and differential thermal analysis (DTA) results are shown in Fig. 3.

According to the TGA curves in Fig. 3(a), all glazed samples show obvious weight loss between 700 and 800 °C, which attribute to the decomposition of dolomite and magnesite. At about 950 °C, the weight loss of all glazed samples was stable. Compared with pure Ag/ZnO, only slight weightlessness of 0.04%, 0.07%, 0.05%, and 0.07% was observed between 1020 and 1200 °C for 0%, 3%, 5%, and 7% Ag/ZnO-loaded samples, respectively. This phenomenon was possibly due to the formation of new crystals with feldspar in raw materials [19]. As the temperature further increased to 1200 °C, the total weight loss of 0%, 3%, 5%, and 7% Ag/ZnO-loaded samples was 11.06%, 10.92%, 10.18%, and 10.92%, respectively. This phenomenon indicated that the addition of ZnO/Ag nanocomposite powder helps to reduce the weightlessness of glaze and effectively reduces the volatilization of oxide in the glaze by forming stable melt substrates [19]. The DTA result in Fig. 3(b) indicated that the glazed sample

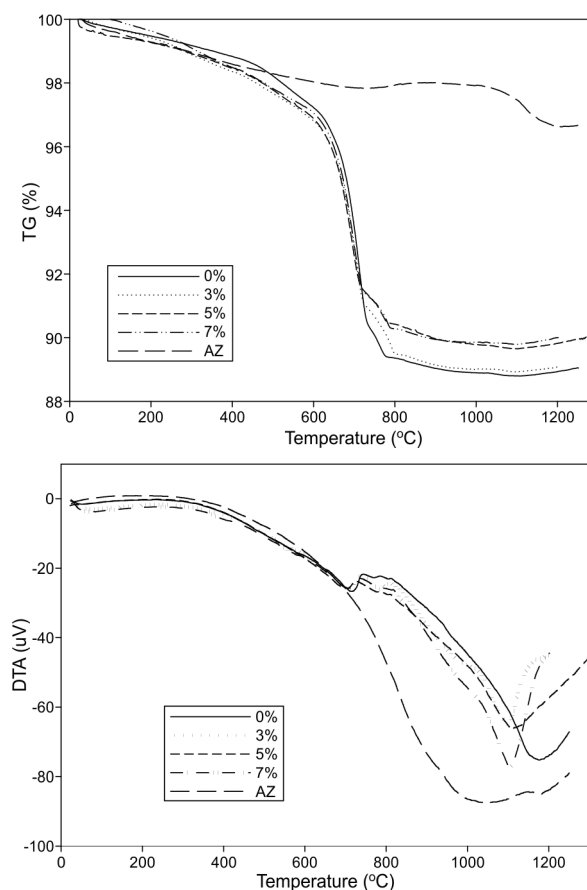


**Fig. 3** TGA and DTA results of ceramic glaze with nano Ag/ZnO addition.

shows an obvious endothermic peak in the temperature range of 1020–1200 °C, which was attributed to the melting of feldspar, such as  $K_2O \cdot Al_2O_3 \cdot 6SiO_2 \rightarrow K_2O \cdot Al_2O_3 \cdot 4SiO_2 + 2SiO_2$  [20,21]. In general, the decomposition temperature of potassium feldspar, sodium feldspar, and calcium feldspar was 1130–1150 °C, 1150–1250 °C, and 1230–1250 °C, respectively [22]. However, the endothermic peaks of 0%, 3%, 5%, and 7% Ag/ZnO-loaded samples were located at 1176, 1112, 1099, and 1104 °C, respectively. These results indicate that the addition of the Ag/ZnO nanocomposite positively affects the reduction in melting temperature of feldspar. With Ag/ZnO loading of 3% and 5%, the melting temperature reduced to about 64 and 77 °C because of the reduced surface energy driving force by the small particle size, high activity, high specific surface area, and surface energy [23].

Except hardness, glazed crack resistance is important for the thermal stability of glazed ceramic. With 0%, 3%, 5%, 7%, and 10% Ag/ZnO loading,

glazed crack resistance was investigated under alternative temperatures at different holding periods. Each experiment was repeated five times to ensure accuracy, and the results are shown in Table 3. These results indicated that glazed crack resistance is enhanced with the increase in sintering temperature and Ag/ZnO loading, since the fusible properties, flexible properties, mechanical strength, and thermal stability of the glaze was improved by the existence of ZnO [9].

Ceramic as a commercial product is greatly dependent on aesthetics [24]. Whiteness is a quality that is crucial for marking, so it was also analyzed under different sintering temperatures with a holding time of 10 min. The result is shown in Fig. 4. With the increase in Ag/ZnO loading, the whiteness of the glaze obviously improved. For this positive effect of Ag/ZnO

**Table 3 Glazed crack resistance under different sintering temperature, holding time, and Ag/ZnO loading**

Sintering temperature–holding time	0%	3%	5%	7%	10%
1050 °C–10 min	1	1	2	2	3
1050 °C–20 min	1	1	2	3	3
1050 °C–30 min	1	2	4	4	4
1100 °C–10 min	1	1	3	3	3
1100 °C–20 min	1	2	4	4	4
1100 °C–30 min	2	3	4	5	5
1130 °C–10 min	1	2	5	5	—
1130 °C–20 min	2	3	5	—	—
1130 °C–30 min	2	4	—	—	—
1150 °C–10 min	3	4	—	—	—
1150 °C–20 min	3	4	—	—	—
1150 °C–30 min	4	5	—	—	—
1170 °C–10 min	4	—	—	—	—
1170 °C–20 min	5	—	—	—	—
1170 °C–30 min	5	—	—	—	—
1190 °C–10 min	—	—	—	—	—
1190 °C–20 min	—	—	—	—	—
1190 °C–30 min	—	—	—	—	—

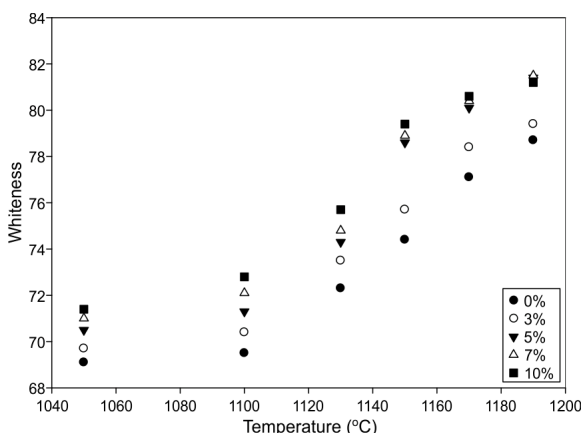


**Fig. 4** Influence on whiteness of ceramic glaze by Ag/ZnO nanocomposite powder.

loading, the positive influence of ZnO on the esthetical property was recognized by other literature [25]. The researching results of Li *et al.* [9] also indicated that the Zn<sup>2+</sup> is favorable for maintaining the silver in the form of the ionic form, and improving the anti-discoloration properties of Ag. The existence of ZnO also improved the fusible properties, flexible properties, mechanical strength, and thermal stability of the glaze, in order to enhance the whiteness and gloss of glaze and widen the preparation conditions under proper loading [9].

In order to clarify the valence state of Ag in ceramic, the range of binding energy from 362 to 384 eV was analyzed by XPS to identify the Ag components. The XPS spectra of Ag–ZnO/ceramic showed a typical Ag 3d signal, corresponding to the binding energy of Ag [26] (Fig. 5), which supported the loading of Ag in glazed ceramic. In Fig. 5, two peaks in the Ag spectrum at 367.5 and 373.8 eV were clearly observed. According to the literature, metallic Ag, which has a typical peak at 368.3 eV, has not been observed [27]. As shown in Fig. 5, the main bond was located at 367.5 eV in the spectrum, which suggested a combined structure of AgO and Ag<sub>2</sub>O as the peaks centered near 367.4 and 367.7 eV were related to AgO and Ag<sub>2</sub>O, respectively [28].

**3.3 Effect on microscopic structures**

The quality of glazed ceramics is independent of its smooth surface. Thus, microscopic structures of glazed ceramics with Ag/ZnO nanocomposite loading were observed under different sizes of Ag/ZnO, sintering temperature, and Ag/ZnO loading.

As shown in Fig. 6, microscopic structures with added ordinary Ag/ZnO and nano-sized Ag/ZnO were analyzed by scanning probe microscopy under a

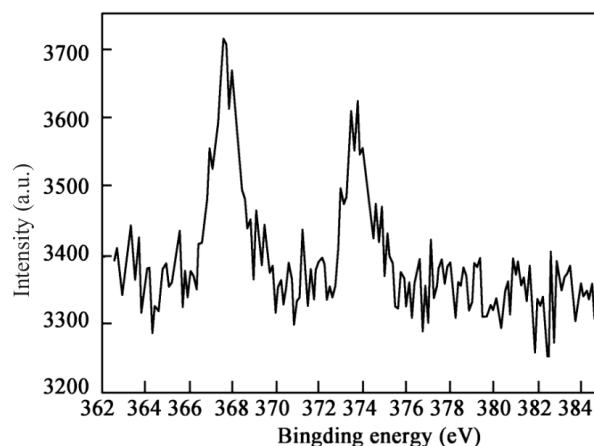


**Fig. 5** XPS spectra of Ag/ZnO decorated ceramic.

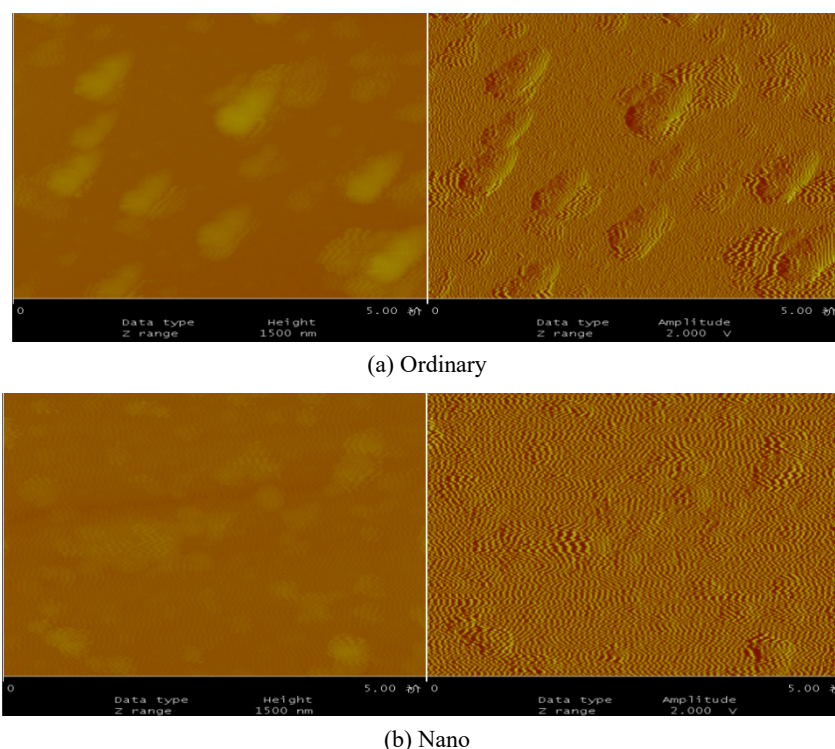


**Fig. 6** Influence on glaze morphology by ordinary and nanometer materials.

sintering temperature of 1150 °C and holding time of 10 min. Compared with ordinary Ag/ZnO, a smooth surface and compact structure were obtained with nano-sized Ag/ZnO loading. This phenomenon possibly resulted from the dispersion of these two materials. With the same Ag/ZnO loading, nano-sized materials were more likely to be homogeneously dispersed in glaze to promote molten as active centers. In general, the Ag/ZnO nanocomposite powder could significantly promote the molten of feldspar and inhibit the formation of large crystals to reduce glaze defects on the surface.

To further confirm the positive effect of nano-sized Ag/ZnO on the microscopic structures, a polarizing microscope was used. As shown in Fig. 7, with ordinary Ag/ZnO loading, many stomata were formed during the ceramic sintering process. The generation of stomata results from the evolution of CO, which is produced by the pyrolysis of billet and glaze. With increased temperature in the sintering process, some stomata would be exhausted because of volume expansion and others would form bubbles in the glaze. According to Zhang *et al.* and Gu *et al.*, the volume percentage of stomata in ceramic can reach 5%–10%, and these stomata are usually distributed in the glassy phase as an isolated state [19,21]. Bubbles can reduce the corrosion resistance and physicochemical properties of the glaze,

and they are unfavorable for glaze sintering. With the addition of nano-sized Ag/ZnO (Fig. 7), only some small bubbles were observed. This phenomenon revealed that the nano sample showed enhanced sintering and molten effects, which promoted bubble expansion and exhaustion.

Given that sintering temperature significantly affects the melting degree, it is clearly vital in glazed ceramic preparation. As shown in Fig. 7, the surface of the glazed ceramic was relatively coarse when 5% Ag/ZnO nanocomposite was added and sintered at 1050 °C. When temperature increased from 1050 to 1150 °C, some spherical defects were clearly observed. However, spherical defects gradually melted when the sintering temperature further increased. According to the results shown in Fig. 3, the component of feldspar in glaze materials decomposed and melted gradually when the sintering temperature increased. Potassium feldspar could decompose and melt under 1150 °C. By contrast, the decomposition temperature of sodium feldspar was 1150–1250 °C. The melting degree of the materials was significant for the microscopic structures of ceramic. High sintering temperature indicated better molten conditions of the raw materials.

In addition, Ag/ZnO loading as a critical factor of economy was investigated to determine the feasibility of the material. With 0%, 3%, 5%, and 7% Ag/ZnO

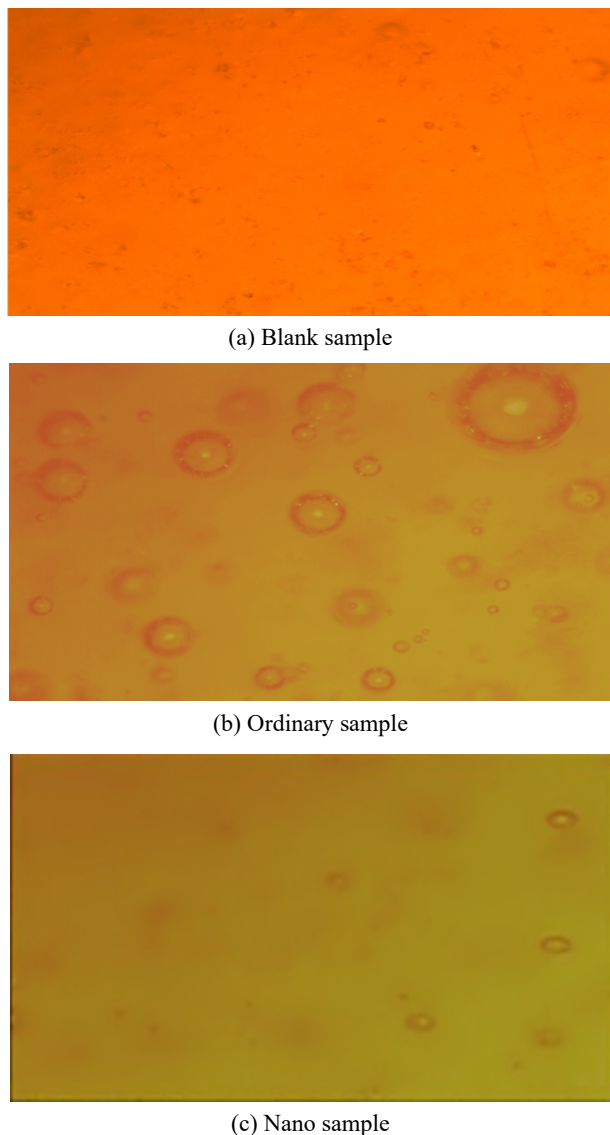


Fig. 7 Observation of bubble in glaze layer.

loading, the ceramic samples were sintered under a sintering temperature of 1150 °C and holding time of 10 min. The glazed surface was then observed via scanning probe microscopy. As shown in Fig. 7(c), the addition of the Ag/ZnO nanocomposite powder exerted obvious effects on glaze morphology. Without the addition of Ag/ZnO nanocomposite, some defects possibly caused by incomplete melted raw materials were clearly observed. With the increase in Ag/ZnO loading, a smoother surface of the glazed ceramic was obtained. This phenomenon was also attributed to the degree of melting [9]. As described in the aforementioned results, the addition of nano-sized Ag/ZnO could decrease the melting temperature of feldspar to smoothen the surface of glazed ceramic. High Ag/ZnO loading could produce effective active

centers and was advantageous for glaze melting.

### 3.4 Effect on antibacterial property

As shown in Fig. 8, the antibacterial property of ceramic was greatly improved by Ag/ZnO nanocomposite loading, and optimal antibacterial activity was obtained with 5% Ag loading against *E.coli*. This phenomenal possibility caused by the small crystallite size (due to the mismatch ionic radii of Ag (1.44 Å) and Zn<sup>2+</sup> (0.74 Å)), positive surface charge (due to the negatively charged bacteria) of Ag/ZnO nanocomposite and the photoactivity of ZnO and the plasmonic effect of silver [29].

Compared with pure ceramic, the antibacterial property of Ag/ZnO-loaded ceramics initially increased with sintering temperature and then decreased. This phenomenon may be due to the free Ag ions on the surface, which significantly affected by the solubility of Ag rather than the concentration [30]. Several studies also reported that the Ag element is consumed by evaporation from ceramic under high sintering temperature [31]. Furthermore, the antibacterial property of ceramic was independent of the holding time in the sintering process. With higher Ag loading, the antibacterial property decreased more rapidly with the holding time because of the evaporation of Ag.

## 4 Conclusions

Given that the addition of nanocomposite can improve the performance of glazed ceramic, this study used several methods for analyses (e.g., TGA, scanning

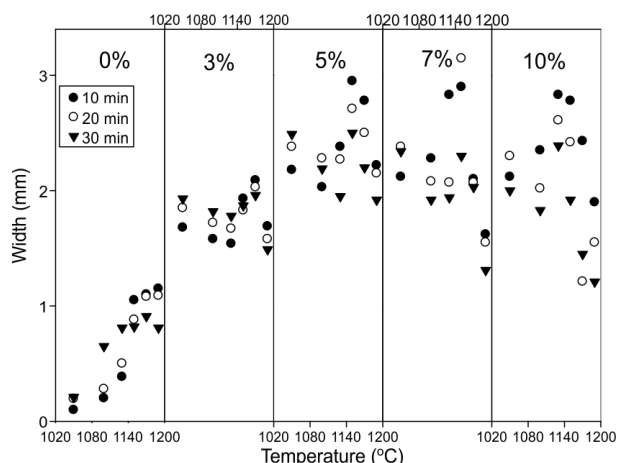


Fig. 8 Antibacterial property of Ag/ZnO decorated ceramic under varied sintering temperature (y axis indicate the width of inhibition zone).



probe microscopy, and polarizing microscopy) to decipher the mechanical properties and microscopic structures of nano Ag/ZnO-added ceramic. In this research, 0%, 3%, 5%, and 7% Ag/ZnO were loaded under different sintering temperatures and holding time for glazed ceramic preparation. The results indicated that the Ag/ZnO nanocomposite powder could significantly promote the melting of glaze and further improve mechanical properties, such as hardness, glaze crack resistance, and whiteness. In addition, enhanced melting performance with Ag/ZnO loading also significantly affected the microscopic structures of glazed ceramic. The increased amount of Ag/ZnO nanocomposite, sintering temperature, and holding time could improve the microscopic structures of glazed ceramics. With the addition of 5% Ag/ZnO nanocomposite under the sintering temperature of 1150 °C and holding time of 10 min, the structure and bubble defects could be greatly reduced. The Ag/ZnO nanocomposite powder could also promote the microstructure of glazed ceramic. This finding not only explains the effect of nanocomposites but also discusses the underlying mechanism. In addition, the antibacterial property of glaze-decorated ceramic with Ag/ZnO loading indicated excellent antibacterial activity against *E.coli* because of the existence of AgO and Ag<sub>2</sub>O.

### Acknowledgements

This work was financially supported by Fujian Province Science and Technology Project Foundation (No. 2017I01010015), and Xiamen Technology Project Foundation (No. 2017S0080).

### References

- [1] Niihara K, Nakahira A, Sekino T, *et al.* Development of ceramic based nanocomposites with high performance. *Journal of the Japan Society of Powder and Powder Metallurgy* 1997, **44**: 887–896.
- [2] Liu N, Xu YD, Li H, *et al.* Effect of nano-micro TiN addition on the microstructure and mechanical properties of TiC based cermets. *J Eur Ceram Soc* 2002, **22**: 2409–2414.
- [3] Zheng Y, Xiong W, Liu W, *et al.* Effect of nano addition on the microstructures and mechanical properties of Ti(C,N)-based cermets. *Ceram Int* 2005, **31**: 165–170.
- [4] Yang W, Shen C, Ji Q, *et al.* Food storage material silver nanoparticles interfere with DNA replication fidelity and bind with DNA. *Nanotechnology* 2009, **20**: 085102.
- [5] Kawashita M, Tsuneyama S, Miyaji F, *et al.* Antibacterial silver-containing silica glass prepared by sol–gel method. *Biomaterials* 2000, **21**: 393–398.
- [6] Lee SM, Lee BS, Byunc TG, *et al.* Preparation and antibacterial activity of silver-doped organic–inorganic hybrid coating on glass substrate. *Colloid Surface A* 2010, **355**: 167–171.
- [7] Baheiraei N, Moztarzadeh F, Hedayati M. Preparation and antibacterial activity of Ag/SiO<sub>2</sub> thin film on glazed ceramic tiles by sol–gel method. *Ceram Int* 2012, **38**: 2921–2925.
- [8] Liu J, Zhang W, Shi H, *et al.* *In situ* plasma fabrication of ceramic-like structure on polymeric implant with enhanced surface hardness, cytocompatibility and antibacterial capability. *J Biomed Mater Res Part A* 2016, **104A**: 1102–1112.
- [9] Li W, Song Y. *Ceramic Additives: Formula, Characteristics, Application*. Beijing: Chemical Industry Press, 2011. (in Chinese)
- [10] Paneto FJ, Pereira JL, Lima JO, *et al.* Effect of porosity on hardness of Al<sub>2</sub>O<sub>3</sub>–Y<sub>3</sub> Al<sub>5</sub>O<sub>12</sub> ceramic composite. *Int J Refract Met H* 2015, **48**: 365–368.
- [11] Ning K, Wang J, Luo D, *et al.* Fabrication and characterization of highly transparent Yb<sup>3+</sup>:Y<sub>2</sub>O<sub>3</sub> ceramics. *Opt Mater* 2015, **50**: 21–24.
- [12] Shen W, Feng L, Feng H, *et al.* Ultrafine silver(II) oxide particles decorated porous ceramic composites for water treatment. *Chem Eng J* 2011, **175**: 592–599.
- [13] Vitale-Brovarone C, Miola M, Balagna C, *et al.* 3D-glass–ceramic scaffolds with antibacterial properties for bone grafting. *Chem Eng J* 2008, **137**: 129–136.
- [14] Lv Y, Liu H, Wang Z, *et al.* Silver nanoparticle-decorated porous ceramic composite for water treatment. *J Membrane Sci* 2009, **331**: 50–56.
- [15] Goei R, Lim T-T. Ag-decorated TiO<sub>2</sub> photocatalytic membrane with hierarchical architecture: Photocatalytic and anti-bacterial activities. *Water Res* 2014, **59**: 207–218.
- [16] Vijayakumar S, Malaikozhundan B, Shanthi S, *et al.* Control of biofilm forming clinically important bacteria by green synthesized ZnO nanoparticles and its ecotoxicity on *Ceriodaphnia cornuta*. *Microb Pathogenesis* 2017, **107**: 88–97.
- [17] Vaseeharan B, Sivakamavalli J, Thaya R. Synthesis and characterization of chitosan-ZnO composite and its antibiofilm activity against aquatic bacteria. *J Compos Mater* 2015, **49**: 177–184.
- [18] Ansari SA, Khan MM, Ansari MO, *et al.* Biogenic synthesis, photocatalytic, and photoelectrochemical performance of Ag–ZnO nanocomposite. *J Phys Chem C* 2013, **117**: 270237–27030.
- [19] Iqbal Y, Lee WE. Microstructural evolution in triaxial porcelain. *J Am Ceram Soc* 2000, **83**: 3121–3127.
- [20] Das SK, Dana K. Differences in densification behaviour of K- and Na-feldspar-containing porcelain bodies. *Thermochimica Acta* 2003, **406**: 199–206.
- [21] Salem A, Jazayeri SH, Rastelli E, *et al.* Dilatometric study of shrinkage during sintering process for porcelain stoneware body in presence of nepheline syenite. *J Mater Process Tech* 2009, **209**: 1240–1246.

- [22] Reifenstein AP, Kahraman H, Coin CDA, *et al.* Behaviour of selected minerals in an improved ash fusion test: Quartz, potassium feldspar, sodium feldspar, kaolinite, illite, calcite, dolomite, siderite, pyrite and apatite. *Fuel* 1999, **78**: 1449–1461.
- [23] Han W, Wang J, Zhang Y, *et al.* The influence of blending the nanophase materials Bi<sub>2</sub>O<sub>3</sub> to the function of ZnO ceramics. *Insulators and Surge Arresters* 2009, **2**: 32–35. (in Chinese)
- [24] Cheng X, Ke S, Wang Q, *et al.* Fabrication and characterization of anorthite-based ceramic using mineral raw materials *Ceram Int* 2012, **38**: 3227–3235.
- [25] Boudeghdegh K, Diella V, Bernasconi A, *et al.* Composition effects on the whiteness and physical-mechanical properties of traditional sanitary-ware glaze. *J Eur Ceram Soc* 2015, **35**: 3735–3741.
- [26] Zhang Z, Zhang J, Zhang B, *et al.* Mussel-inspired functionalization of graphene for synthesizing Ag-polydopamine-graphene nanosheets as antibacterial materials. *Nanoscale* 2013, **5**: 118–123.
- [27] Zheng J, Lin H, Wang Y, *et al.* Efficient low-temperature selective hydrogenation of esters on bimetallic Au–Ag/SBA-15 catalyst. *J Catal* 2013, **297**: 110–118.
- [28] Sandoval A, Delannoy L, Méthivier C, *et al.* Synergetic effect in bimetallic Au–Ag/TiO<sub>2</sub> catalysts for CO oxidation: New insights from in situ characterization. *Appl Catal A: Gen* 2015, **504**: 287–294.
- [29] Abinaya C, Marikkannan M, Manikandan M, *et al.* Structural and optical characterization and efficacy of hydrothermal synthesized Cu and Ag doped zinc oxide nanoplate bactericides. *Mater Chem Phys* 2016, **184**: 172–182.
- [30] Li ZJ, Wei C, Guo F, *et al.* Studying on the dispersion and performances of ZnO/Ag nanocomposite antibacterial agent. *J Funct Mater Devic* 2007, **38**: 3430–3432. (in Chinese)
- [31] Range S, Hagemeyer D, Rotan O, *et al.* A continuous method to prepare poorly crystalline silver-doped calcium phosphate ceramics with antibacterial properties. *RSC Adv* 2015, **5**: 43172–43177.

**Open Access** The articles published in this journal are distributed under the terms of the Creative Commons Attribution 4.0 International License (<http://creativecommons.org/licenses/by/4.0/>), which permits unrestricted use, distribution, and reproduction in any medium, provided you give appropriate credit to the original author(s) and the source, provide a link to the Creative Commons license, and indicate if changes were made.